Vps11, a subunit of the tethering complexes HOPS and CORVET, is involved in regulation of glycolipid degradation and retrograde toxin transport

Audun Sverre Kvalvaag[1,2,3], Sascha Pust[1,3], and Kirsten Sandvig[1,2,3,*]

[1]Department of Biochemistry; Institute for Cancer Research; The Norwegian Radium Hospital; Oslo University Hospital; Montebello, Oslo, Norway; [2]Department of Biosciences; Faculty of Mathematics and Natural Sciences; University of Oslo; Oslo, Norway; [3]Centre for Cancer Biomedicine; Faculty of Medicine; University of Oslo; Montebello, Oslo, Norway

We recently reported that ERM (ezrin, radixin, moesin) proteins are involved in intracellular sorting of Shiga toxin (Stx) and its receptor globotriaosylceramide (Gb3), and that depletion of ezrin and moesin reduced retrograde Golgi transport of Stx. In the same study, we found that knockdown of Vps11, a core subunit of both the homotypic fusion and protein sorting (HOPS) complex and the class C core vacuole/endosome tethering factor (CORVET), increased retrograde transport of Stx and could counteract the inhibiting effect of moesin and ezrin knockdown. In this study we demonstrate that Vps11 knockdown also leads to increased Stx toxicity as well as increased retrograde transport and toxicity of ricin. Additionally, we show that knockdown of Vps11 restores the reduced Gb3 level observed after moesin depletion.

Vesicular transport along the endocytic pathway involves such processes as endosomal maturation and fusion with lysosomes. During this transport, a myriad of mechanisms act in concert to ensure that the vesicle content is sorted correctly. Governing several of these mechanisms are the endosomal tethering complexes CORVET and HOPS, both built on the same Vps-C core. In yeast, the core consists of the subunits Vps11, Vps16, Vps18 and Vps33. The CORVET complex is defined by the two accessory subunits Vps3 and Vps8, while the HOPS complex is defined by the accessory proteins Vps39 and Vps41. Both complexes are evolutionary conserved and homologs have been found in mammals (for reviews see (1,2)). Among their interaction partners are the ERM proteins, which have been shown to associate with the core subunit Vps11 (3). ERM proteins are known as organizers of the plasma membrane and connect transmembrane and membrane associated proteins with the cortical actin cytoskeleton. ERM proteins are recruited to the plasma membrane by phosphatidylinositol 4,5-bisphosphate (PIP2) where they are activated and stabilized by phosphorylation. Several reports suggest that ERM proteins are involved in confining components in lipid rafts, including glycosphingolipids such as the Stx receptor Gb3, by anchoring picket proteins surrounding the rafts to actin filaments (4,5). Furthermore, ERM proteins have been shown to be involved in recycling of transmembrane proteins such as adrenergic receptors (6,7), NHE3 (8) and the transferrin receptor (9).

We have previously demonstrated that moesin depletion inhibits retrograde Shiga toxin transport and reduces the cellular level of Gb3, shown both by HPTLC and immunolabeling (10). As Vps11 knockdown could counteract the inhibiting effect on retrograde Stx transport, we asked whether the same was true for the Gb3 level. HeLa cells were immunostained for Gb3 and analyzed by scan^R microscopy as described earlier (10). **Figure 1A** shows co-localization between moesin and surface Gb3, indicating that they exist in the same plasma membrane domains, albeit on different leaflets as Gb3 is known to be exclusively localized in the outer leaflet and moesin is cytosolic and without transmembrane domains. Permeabilization of cells immunolabeled for Gb3 did not significantly alter the Gb3 distribution (Supplementary Figure 1). **Figure 1B** shows how the level of total cellular Gb3 was reduced by ~20% after moesin knockdown and restored after double knockdown of moesin and Vps11. Knockdown of Vps11 alone did not seem to affect the Gb3 level. P-glycoprotein (P-gp) is an ABC drug transporter involved in the translocation of the Gb3 precursor glucosylceramide into the Golgi apparatus where it is processed to more complex glycosphingolipids (11). P-gp expression has been linked with ERM protein expression and activation (12), but the P-gp level was not altered in response to moesin depletion (**Fig. 1C**). These results suggest that knockdown of moesin increases degradation of Gb3 and that the degradation is inhibited by Vps11 knockdown.

Furthermore, we investigated whether Stx toxicity was enhanced as a consequence of the increased retrograde Stx transport observed after Vps11 knockdown. Indeed, Stx mediated inhibition of protein synthesis was stronger after Vps11 depletion (**Fig. 2A**). In contrast to Stx, which binds specifically to Gb3 on
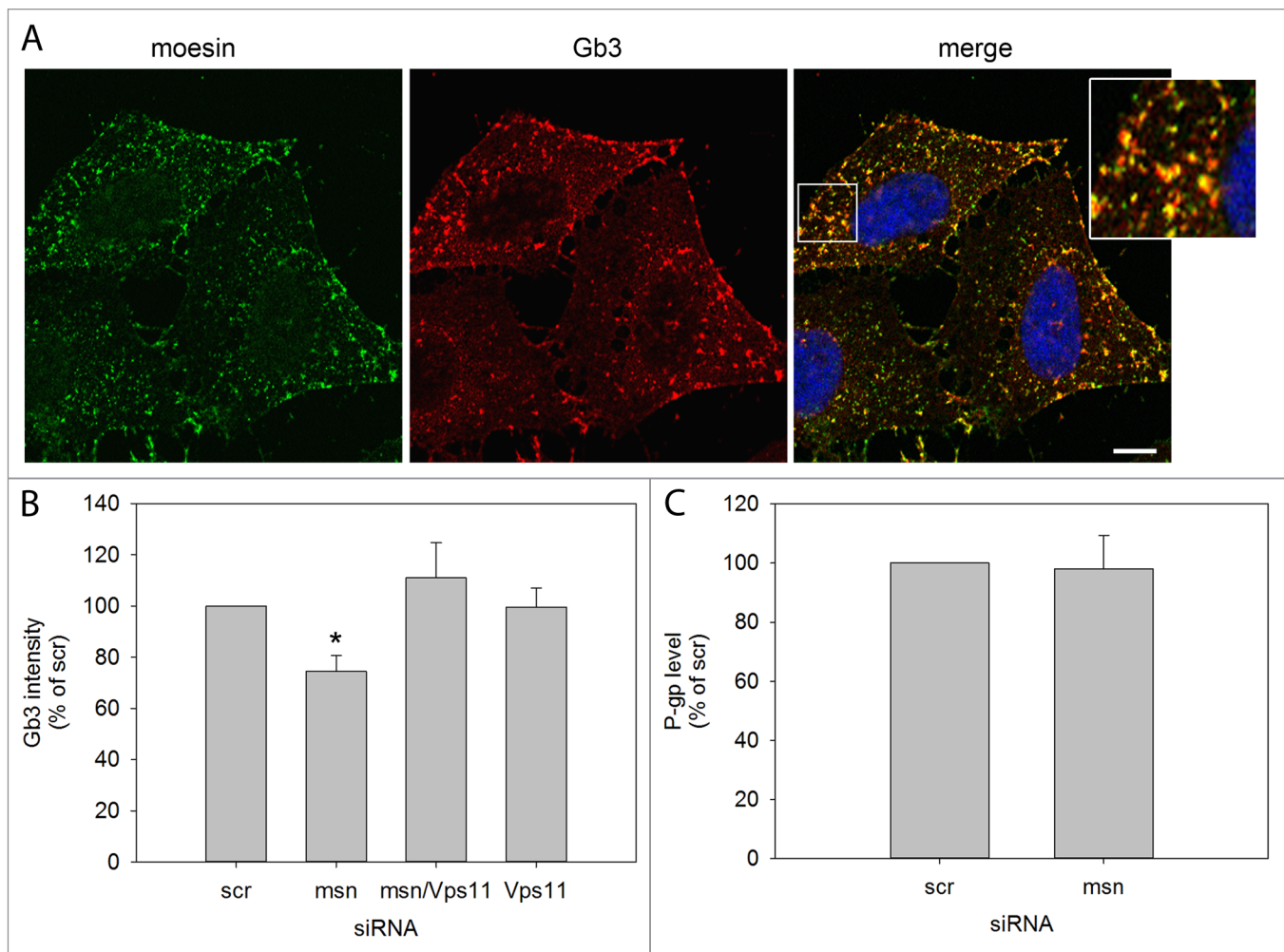
Figure 1. The level of Gb3 is reduced after moesin knockdown and restored after moesin and Vps11 double knockdown. (A) HeLa cells were incubated for 20 min on ice with an anti Gb3 antibody before they were fixed in 4% paraformaldehyde (PFA), permeabilized with 0.1% Tx-100 for 2 min and immunolabeled for moesin. Representative micrographs of optical sections of 0.7 μm displaying immunolabeled moesin in the left panel, immunolabeled Gb3 in the middle panel and a merged image with a magnified inlay in the right panel are shown. Scale bar represents 10 μm. (B) Quantification of the fluorescent intensity of total cellular Gb3 immunostained in fixed and permeabilized cells depleted of moesin (msn) and Vps11 compared with cells treated with scrambled siRNA. Micrographs were obtained by high throughput microscopy of > 1000 cells per condition with an automated scan^R microscope and fluorescent intensity was analyzed by scan^R software (mean intensity ± SEM; scr, msn, msn/Vps11; n = 4, Vps11; n = 2, *P = 0.0253). (C) Quantification of the P-gp level obtained by western blotting in moesin knockdown cells compared with scrambled siRNA treated cells (mean ± SEM, n = 3).

the surface of cells, the plant toxin ricin binds promiscuously to glycolipids and glycoproteins with a terminal galactose (13,14). It is therefore endocytosed through a wide range of mechanisms before the toxin is transported retrogradely to the Golgi apparatus and the ER from where the toxic A subunit is translocated into the cytosol and inhibits protein synthesis (for reviews see (13,14)). To assess the involvement of Vps11 in retrograde transport of ricin, we measured ricin sulfation and ricin toxicity after Vps11 knockdown. Eligible proteins are sulfated in the Golgi and by incubating cells with a ricin construct modified with sulfation and glycosylation sites, ricin-sulf2 (rs2), in the presence of radioactively labeled sulfate, we could measure the toxin fraction having reached the Golgi apparatus. We could also separate it from the fraction having passed through the Golgi and arrived at the ER because of a size increase resulting from addition of an oligosaccharide to the toxin construct by ER localized oligosaccharyltransferases. Vps11 depletion led to increased sulfation and glycosylation of rs2 and increased ricin mediated inhibition of protein synthesis (**Fig. 2B-C**). The difference between sulfated and glycosylated rs2 is not significant, indicating that Vps11 is not involved in Golgi to ER transport. Given its ubiquitous uptake, ricin is prone to undertake a variety of transport routes from endosomes to the Golgi, while Stx seems to follow a different and more specific path. The observation that Vps11 depletion affects transport of both toxins thereby underlines the functional range of Vps-C core complexes in protein sorting.

Taken together, these results suggest that the interplay between moesin and Vps11 is important in glycolipid homeostasis, and that the level of retrograde protein transport increases in the absence of functional CORVET and HOPS complexes.
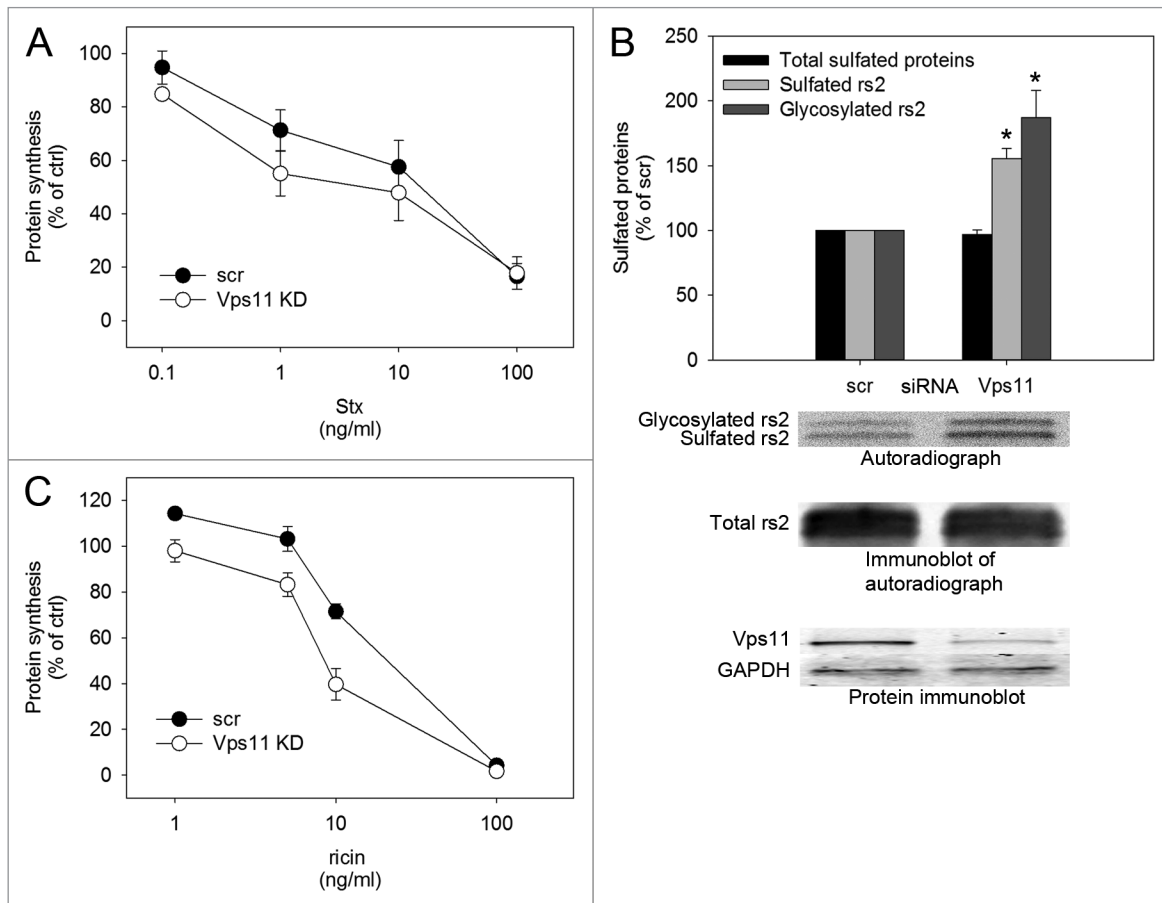
Figure 2. Retrograde transport and toxicity of Shiga toxin and ricin is increased in response to Vps11 knockdown. (A) HeLa cells were incubated with Stx concentrations ranging from 0.1 ng/ml to 100 ng/ml for 5.5 h. The toxicity in scrambled and Vps11 siRNA treated cells was analyzed by measuring the level of protein synthesis in Stx treated cells compared with control cells without toxin treatment (ctrl) (mean ± SEM, n = 4, P = 0.0118 at 1 ng/ml Stx). (B) HeLa cells were incubated with ricin-sulf2 (rs2) for 2 h in the presence of $^{35}SO_4^{2-}$ and the amount of sulfated rs2 was quantified on autoradiographs with Quantity One® software (mean ± SEM, n = 3, sulfated rs2; *P = 0.003, glycosylated rs2; *P = 0.0316). Representative blots are depicted below the graph. (C) HeLa cells were incubated with ricin concentrations ranging from 1 ng/ml to 100 ng/ml for 3 h and the toxicity was analyzed as described for Stx in (A) (mean ± SEM, n = 3, P = 0.0299 at 1 ng/ml ricin).

Materials and Methods

Sulfation of ricin-sulf2

HeLa cells were incubated with 0.2 mCi/ml $Na_2^{35}SO_4$ for 3 h in a humidified 5% CO_2 atmosphere at 37 °C before ~2 µg/ml ricin-sulf2 (rs2) was added and the cells were grown for two more h. The cells were washed and lysed (100 mM NaCl, 10 mM Na_2HPO_4, 1 mM EDTA, 1% v/v Triton X-100, 60 mM n-octyl-β-D-glucopyranoside, protease inhibitor (Roche)). The nuclear fraction was removed by centrifugation at 6800 g before rs2 was immunoprecipitated with Protein A Sepharose beads (GE healthcare). Proteins in the supernatant were precipitated with 5% w/v trichloroacetic acid (TCA) and dissolved in 0.1 M KOH before their total β-radiation was measured on a β-counter (Packard). The immunoprecipitate was washed twice in 0.35% v/v Triton X-100 in PBS, incubated for 5 min in sample buffer (0.063 M TRIS-HCl, 2% w/v SDS, 0.0025% w/v bromphenol blue, 10% v/v glycerol in H_2O) at 95 °C and run on a 4–20% SDS-PAGE gel. The proteins were transferred to Immobilon PVDF-FL membranes (Millipore), visualized by autoradiography and quantified with Quantity One® software (Bio-Rad).

Toxicity assay

HeLa cells were incubated with 1 x 10^{-4} µg/ml to 1 x 10^{-1} µg/ml Shiga toxin or 1 x 10^{-3} µg/ml to 1 x 10^{-1} µg/ml ricin for 5.5 h and 3 h, respectively. Then the cells were incubated with 2 µCi/ml [^{3}H]leucine for 15 min before proteins were precipitated by washing the cells twice with 5% TCA for 5 min. Finally, the proteins were dissolved in 0.1 M KOH and the radioactivity was measured by using a β-counter (Packard).

Statistics

Statistical significance was tested using Student's *t* test for all experiments performed three times or more. A p-value of 0.05 or less was regarded as statistically significant.

Disclosure of Potential Conflicts of Interest

No potential conflicts of interest were disclosed.

References

1. Nickerson DP, Brett CL, Merz AJ. Vps-C complexes: gatekeepers of endolysosomal traffic. Curr Opin Cell Biol 2009; 21:543-51; PMID:19577915; http://dx.doi.org/10.1016/j.ceb.2009.05.007

2. Solinger JA, Spang A. Tethering complexes in the endocytic pathway: CORVET and HOPS. FEBS J 2013; 280:2743-57; PMID:23351085; http://dx.doi.org/10.1111/febs.12151

3. Chirivino D, Del Maestro L, Formstecher E, Hupé P, Raposo G, Louvard D, Arpin M. The ERM proteins interact with the HOPS complex to regulate the maturation of endosomes. Mol Biol Cell 2011; 22:375-85; PMID:21148287; http://dx.doi.org/10.1091/mbc.E10-09-0796

4. Itoh K, Sakakibara M, Yamasaki S, Takeuchi A, Arase H, Miyazaki M, Nakajima N, Okada M, Saito T. Cutting edge: negative regulation of immune synapse formation by anchoring lipid raft to cytoskeleton through Cbp-EBP50-ERM assembly. J Immunol 2002; 168:541-4; PMID:11777944

5. Gupta N, Wollscheid B, Watts JD, Scheer B, Aebersold R, DeFranco AL. Quantitative proteomic analysis of B cell lipid rafts reveals that ezrin regulates antigen receptor-mediated lipid raft dynamics. Nat Immunol 2006; 7:625-33; PMID:16648854; http://dx.doi.org/10.1038/ni1337

6. Cao TT, Deacon HW, Reczek D, Bretscher A, von Zastrow M. A kinase-regulated PDZ-domain interaction controls endocytic sorting of the beta2-adrenergic receptor. Nature 1999; 401:286-90; PMID:10499588; http://dx.doi.org/10.1038/45816

7. Stanasila L, Abuin L, Diviani D, Cotecchia S. Ezrin directly interacts with the alpha1b-adrenergic receptor and plays a role in receptor recycling. J Biol Chem 2006; 281:4354-63; PMID:16352594; http://dx.doi.org/10.1074/jbc.M511989200

8. Zhao H, Shiue H, Palkon S, Wang Y, Cullinan P, Burkhardt JK, Musch MW, Chang EB, Turner JR. Ezrin regulates NHE3 translocation and activation after Na+-glucose cotransport. Proc Natl Acad Sci U S A 2004; 101:9485-90; PMID:15197272; http://dx.doi.org/10.1073/pnas.0308400101

9. Barroso-González J, Machado JD, García-Expósito L, Valenzuela-Fernández A. Moesin regulates the trafficking of nascent clathrin-coated vesicles. J Biol Chem 2009; 284:2419-34; PMID:19047065; http://dx.doi.org/10.1074/jbc.M805311200

10. Kvalvaag AS, Pust S, Sundet KI, Engedal N, Simm R, Sandvig K. The ERM proteins ezrin and moesin regulate retrograde Shiga toxin transport. Traffic 2013; 14:839-52; PMID:23593995; http://dx.doi.org/10.1111/tra.12077

11. De Rosa MF, Ackerley C, Wang B, Ito S, Clarke DM, Lingwood C. Inhibition of multidrug resistance by adamantylgb3, a globotriaosylceramide analog. J Biol Chem 2008; 283:4501-11; PMID:18003606; http://dx.doi.org/10.1074/jbc.M705473200

12. Kano T, Wada S, Morimoto K, Kato Y, Ogihara T. Effect of knockdown of ezrin, radixin, and moesin on P-glycoprotein function in HepG2 cells. J Pharm Sci 2011; 100:5308-14; PMID:21837648; http://dx.doi.org/10.1002/jps.22718

13. Sandvig K, Torgersen ML, Engedal N, Skotland T, Iversen TG. Protein toxins from plants and bacteria: probes for intracellular transport and tools in medicine. FEBS Lett 2010; 584:2626-34; PMID:20385131; http://dx.doi.org/10.1016/j.febslet.2010.04.008

14. Sandvig K, Skotland T, van Deurs B, Klokk TI. Retrograde transport of protein toxins through the Golgi apparatus. Histochem Cell Biol 2013; 140:317-26; PMID:23765164; http://dx.doi.org/10.1007/s00418-013-1111-z